Unconventional magnetism in semiconductors: Role of localized acceptor states

Pratibha Dev and Peihong Zhang
Department of Physics, University at Buffalo–State University of New York, Buffalo, New York 14260, USA
(Received 9 September 2009; revised manuscript received 24 November 2009; published 8 February 2010)

Magnetism induced by the localized defect states in the otherwise "nonmagnetic" *sp* semiconductors—GaN and ZnO—is investigated using *ab initio* methods. The defects studied include the cation vacancy in ZnO, a potassium substitutional in GaN, and an acceptor like defect complex (gallium vacancy along with oxygen as an anion substitutional). In all three cases, spontaneous spin-polarized ground states are obtained within density-functional theory (DFT). Magnetic coupling between defect-induced local moments is also studied by mapping the DFT total energy to a nearest-neighbor Heisenberg model. The coupling between magnetic moments is found to be ferromagnetic for the case of cation vacancies in ZnO. This is also found to be the case for the potassium substitutional in GaN. However, the magnetic coupling is antiferromagnetic for the acceptorlike defect complex. A kinetic exchange model is used to explain this diverse magnetic behavior shown by the different systems.

DOI: 10.1103/PhysRevB.81.085207 PACS number(s): 75.50.Pp, 71.15.Mb, 71.55.−i, 75.10.−b

I. INTRODUCTION

For its practical application, the field of spintronics requires room-temperature ferromagnetic semiconductors.[1,2] This need has spurred a tremendous amount of experimental and theoretical research in quest for high-T_C dilute magnetic semiconductors (DMSs). A large body of the work on DMS has focused on (Ga,Mn)As and (In,Mn)As systems. Unfortunately, the highest T_C reported (160–170 K) (Ref. 3) is still far below room temperature. Since the work of Dietl *et al.*,[2] wide-gap semiconductors such as GaN and ZnO based DMS have attracted much research attention.[4] However, experiments have revealed a multitude of complex properties in these doped systems, such as a wide range of T_C (Refs. 5–11) and diverse magnetic properties ranging from ferromagnetic[5–9] to spin glass[12] and paramagnetic[13] behaviors.

On the theory side, in spite of tremendous research activities, fundamental magnetism in GaN- and ZnO-based DMS is still not well understood. In particular, the role that defect states play in mediating the magnetic coupling[14–19] and in promoting the observed magnetism remains to be thoroughly investigated. The difficulties in the synthesis of the room-temperature DMS and the incomplete understanding of the underlying exchange mechanism have, in turn, resulted in a renewed interest in the problems of local-moment formation and collective magnetism in solids.

Magnetism in solids is conventionally associated with the highly localized unpaired electrons in 3*d* and 4*f* states of the transition or rare-earth metals. Owing to their localization and high degree of degeneracy, the intra-atomic exchange effects (Hund's rule mechanism) may dominate even in the solid environment, resulting in the formation of local magnetic moment in solids.[20] Interestingly, the 2*p* electrons of the second row elements—carbon, nitrogen, and oxygen—also share the similar property, *viz.*, the localized nature of the electrons in those states. Figure 1 compares and shows the similar localization behavior of the atomic radial wavefunctions of oxygen 2*p* and manganese 3*d* states. Since the valence states of ZnO and GaN are derived from these fairly localized oxygen or nitrogen *sp* states, one can then expect that unpaired electrons in acceptor states would favor a spin-polarized configuration[14,21–23] and give rise to local-moment formation.

On the other hand, compared to the 3*d* state of transition metals, these defect states are more extended, which may result in long-ranged magnetic coupling. Therefore, this duality (localization vs. extension) of the defect states opens up the possibility of defects induced and/or mediated magnetism in these systems.[23–26] When magnetic ions are introduced, these defect states are expected to play an important role in mediating their magnetic interactions.

Indeed, recent work in this field points toward the possibility of a new class of ferromagnetic semiconductors based on the sp/d^0 materials. This has been observed in both organic and inorganic materials such as oxides and nitrides. One important aspect that all such experimental reports[27–37] and theoretical studies[24,38–43] have in common is the presence of defects in the host matrix, providing the possibility of forming open shell electronic configurations. The two conditions—open shell configuration as well as the localization of the defect states—are the prerequisites to the local magnetic-moment formation in these otherwise nonmagnetic materials. In future, advances in material-synthesis and post-

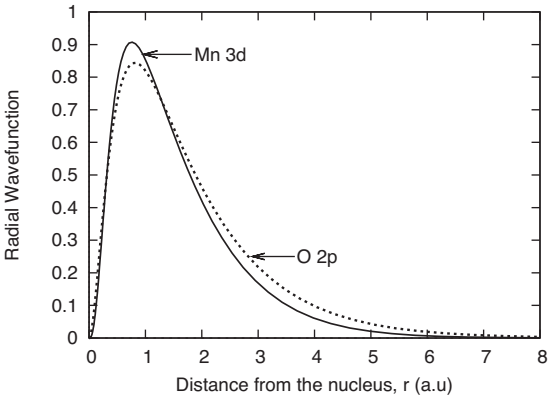

FIG. 1. A comparison between the oxygen 2*p* and manganese 3*d* states.

processing techniques may lead to more accurate defect manipulation and engineering and the sp/d^0-magnetic materials might become a promising alternative to the transition-metal-doped semiconductors. It is, therefore, imperative to understand the defect-induced and defect-mediated magnetisms at the microscopic level.

In a recent study[23] (from here on referred to as *paper I*), the authors have focused on the intrinsic defect-induced magnetism in wide-gap nitrides. In this paper, we extend our work to include defect-induced magnetism in ZnO. We also expand the scope of this work by studying the magnetic properties of a nonmagnetic substitutional and a defect complex in GaN. Through this extensive (though, by no means an exhaustive) study, we wish to emphasize that the introduction of (uncompensated or partially compensated) deep-acceptor states might lead to the local-moment formation in these otherwise nonmagnetic nitrides and oxides. Recent works on calcium-doped GaN,[44] nitrogen-doped ZnO,[45] and carbon-doped ZnO,[36] to name a few, also support this view. Magnetic coupling between these defect-induced moments, on the other hand, is a result of delicate interplay between localization, defect charge states, and Jahn-Teller distortions.

This paper is organized as follows. Section II discusses the computational details of this work. In Sec. III, we report the magnetic properties of the neutral and charged cation vacancies in ZnO. Magnetic exchange mechanism between defect-induced moments in the defective structure is also discussed. Section IV focuses on the cation substitution in GaN while Sec. V focuses on the defect complex $[V_{Ga}\text{-}O_N]$ in GaN. Although these two systems display different magnetic behaviors, they can again be explained using the same exchange model. The last section (Sec. VI) is the discussion.

II. CALCULATION DETAILS

The results presented here are for the cubic (zinc-blende structure) ZnO and GaN. This is done for the sake of simplicity and for comparison to the results obtained for cation vacancy in cubic GaN that were reported in paper I. Our first-principles calculations are based on density-functional theory (DFT) within the generalized gradient approximation (GGA).[46] The Perdew-Burke-Ernzerhof[47] functional is used to account for the exchange-correlation effects. All calculations are carried out using the QUANTUM-ESPRESSO package.[48]

Depending on the system under consideration, we used either the norm conserving[49] or ultrasoft[50] pseudopotentials. For ZnO, since the zinc $3d$-semicore states are included explicitly in the calculation, we use ultrasoft pseudopotentials. For GaN systems, norm-conserving pseudopotentials are used. The cut-off energies for the plane-wave expansion are carefully tested to ensure the convergence of the calculations. The k-point set was generated by the Monkhorst-Pack scheme[51] with a $6\times6\times6$ k grid for a 64 atom supercell. We use the experimental lattice constants[52,53] and all atomic positions are fully relaxed when defects are introduced. In all cases, the relaxation threshold is set to be better than 10^{-4} Ry/a.u. for the forces.

It is well known that the GGA [or the local-density approximation (LDA)] underestimates the band gap for most semiconductors and insulators. This "band-gap problem" is usually not a serious issue for studying the ground-state properties. However, the band-gap underestimation might lead to erroneous results when studying defect properties. This is especially true for the case of ZnO. Within the GGA, the band gap of bulk ZnO was grievously underestimated to be about 0.66 eV. When defects are introduced, this greatly reduced gap could result in a wrong placement of the defect states. The severe underestimation of the band gap of ZnO can be traced to the inadequate treatment of the semicore electrons by the GGA (or the LDA). Within the GGA, the zinc $3d$ states are located around 5 ± 1 eV below the valence-band maximum (VBM). This is more than 2 eV too shallow compared to the measured value of 7.5–8.8 eV.[54,55] Consequently, strongly enhanced pd hybridization occurs, which pushes the occupied valence states up and results in a greatly reduced band gap. Due to the wrong placement of the defect states within the band gap, a cation vacancy in a fully relaxed structure gives rise to a smaller local magnetic moment than the expected value of $2.00\mu_B$. To remedy this problem, we incorporate an effective on-site Coulomb interaction ($U=7$ eV) for the cation d states using the GGA+U method.[56] The GGA+U method gives a more reasonable value (~1.02 eV) for the band gap of ZnO and we believe it will give better results for defect properties than the GGA.

III. CATION VACANCIES IN ZnO

We first study the magnetic properties of zinc vacancy in ZnO. Several authors[26,57–59] have pointed out to the cation vacancies as the possible source of the localized moments and ferromagnetic behavior in undoped oxides. In particular, positron-annihilation spectroscopy measurements[59] suggest that the ferromagnetism observed in undoped ZnO films is related to Zn vacancies. As mentioned in Sec. I, the top valence states of ZnO are derived from the oxygen $2p$ states that are substantially localized. Therefore, similar to the case of cation vacancy-induced magnetic moment in GaN, one expects moment formation to result from the zinc vacancies in ZnO.

After removing a Zn atom in a 64-atom supercell, all atoms are fully relaxed within GGA+U while keeping the lattice parameter fixed at the experimental value. The relaxation energy, defined as the total-energy difference between the relaxed structure and the unrelaxed structure in which all atoms are in the ideal bulk positions, is about 0.34 eV. In the relaxed defective structure, oxygen atoms surrounding the neutral Zn vacancy moved outward by 0.16 Å while Zn-O bond length in the first shell around the vacancy reduced from 1.99 to 1.93 Å.

Figure 2 shows the spin-resolved density of states (DOS) of a 64-atom ZnO supercell containing a neutral Zn vacancy $[Zn_{31}(V_{Zn})O_{32}]$. In spite of the spurious broadening of the defect states (owing to the overlap of defect states as a result of the relatively small supercell used in the calculation), the unoccupied minority-spin states are nearly completely separated from the bulk valence states, resulting in the formation of $2.0\mu_B$ local moment. The formation of a $2.0\mu_B$ local moment by a Zn vacancy can be easily understood: A neutral

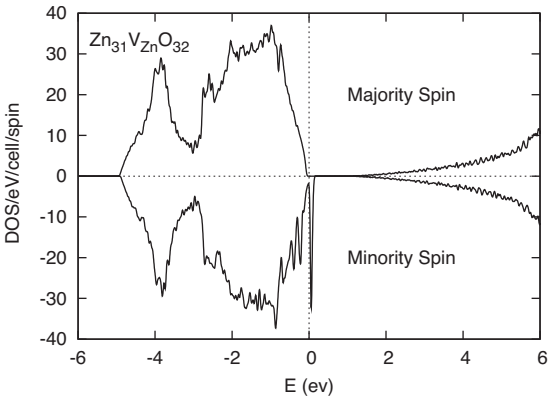

FIG. 2. Spin-resolved density of states of a Zn vacancy in a 64-atom ZnO supercell.

cation vacancy in ZnO results in six quasi localized electrons in the dangling bonds on the oxygen atoms surrounding the vacancy. Under the influence of the cubic crystal field (which has the T_d symmetry), the defect states are split into a singlet a_1 state and a triplet t_2 state. The fully occupied a_1 state lies much below the Fermi energy and so in the rest of this section we will only concern ourselves with the t_2 state. Due to spin polarization, the triplet state splits into majority-spin $t_2^{\uparrow\uparrow\uparrow}$ and minority-spin $t_2^{\downarrow}$ states. This results in the formation of a net local moment of $2.0\mu_B$. The calculated spin-polarization energy, ΔE^{pol}, which is defined as the energy difference between the spin-unpolarized and the spin-polarized states, is about 0.16 eV per defect site.

In order to find the nature of the magnetic coupling between the defect-induced local moments, we double the size of the supercell. The 128-atom supercell contains two 64-atom cells adjacent to each other. A cation vacancy is introduced in each of these adjoining cells. Depending on the initial conditions of the self-consistent field calculations, the magnetic structure can be made either ferromagnetic (FM) or antiferromagnetic (AFM). If there is a magnetic coupling between the defect-induced local moments, different magnetic structures will have different total energies. We define the magnetic energy difference ΔE^M as the total-energy difference between the AFM and the FM structures, i.e., $\Delta E^M = E^{\text{AFM}} - E^{\text{FM}}$. From the total energies calculated within GGA+U method, we find that the structure with ferromagnetically aligned magnetic moments (induced by the neutral zinc vacancies) has a lower energy, as shown in Table I.

A convenient way to study the magnetic interaction is to map the total energy of the magnetic system to a Heisenberg model

$$H = -\sum_{\langle ij \rangle} J_{ij} \mathbf{S_i} \cdot \mathbf{S_j}. \tag{1}$$

Only the nearest-neighbor (NN) interactions are considered in this work. For the case of FM alignment of defect-induced moments, there are six NNs with aligned spins. The magnetic energy (for the 128-atom supercell) is

TABLE I. Magnetic properties of Zn vacancy in ZnO. The results for cation vacancy in GaN (see paper I for details) are included for comparison. The magnetic energy difference is defined in Eq. (4). The spin-polarization energy is for one defect.

System	Charge state	m (μ_B)	ΔE^M (meV)	J_0 (meV)	ΔE^{pol} (meV)
ZnO: V_{Zn}	0	2.0	77	19	164
	−1	1.0	27	27	54
GaN: V_{Ga}	−1	2.0	122	31	256
	−2	1.0	27	27	64

$$E^{\text{FM}} = -6J_0S^2, \tag{2}$$

where S is the total spin and J_0 is the exchange parameter. In the AFM case, there are four nearest neighbors with aligned spins and two nearest neighbors with antialigned spins. Therefore, the magnetic energy is

$$E^{\text{AFM}} = -(4J_0 - 2J_0)S^2 = -2J_0S^2. \tag{3}$$

From the magnetic energy expressions in Eqs. (2) and (3), one can calculate the energy difference between the two spin alignments

$$\Delta E^{\mathbf{M}} = E^{\text{AFM}} - E^{\text{FM}} = 4J_0S^2. \tag{4}$$

The first-principles calculations yield the left-hand side of Eq. (4) and these numbers are then used to calculate the exchange parameters J_0, listed in Table I. Since the cation vacancies can exist in several charge states, we have also studied negatively charged defect. These results are also summarized in Table I. Charging the defect with one electron reduces the local moment to $1.0\mu_B$. The magnetic coupling, however, remains ferromagnetic. For comparison, we have also included the results of the exchange parameters for various charge states of cation vacancy defects in GaN.[23] Note that the magnetic properties of neutral Zn vacancies (V_{Zn}) are to be compared to those of (V_{Ga}^{-}). Similarly, the magnetic properties of (V_{Zn}^{-}) are to be compared to those of (V_{Ga}^{2-}). From Table I, one can see that the calculated values of the exchange parameter are substantial for both charge states. However, quantum fluctuations and also disorder effects may reduce the effective magnetic coupling,[60] although the effects may be stronger in lower-dimensional systems. Even if the exchange parameters are reduced by 20% from our current estimates, these couplings are still surprisingly strong and long ranged.

In paper I, we described the kinetic exchange mechanism to explain the magnetic coupling between defect-induced local moments. The same mechanism also explains the results obtained for ZnO. The energy-level diagram in Fig. 3 helps to illustrate the mechanism. For simplicity, the diagram contains only the partially filled t_2 states. The triply-degenerate majority-spin states are completely filled while the minority-spin states are only partially filled. As shown in the diagram, for both neutral and the negatively charged cation vacancies, the parallel spin alignment allows for the virtual hopping between the electrons in the defect states (thereby, lowering

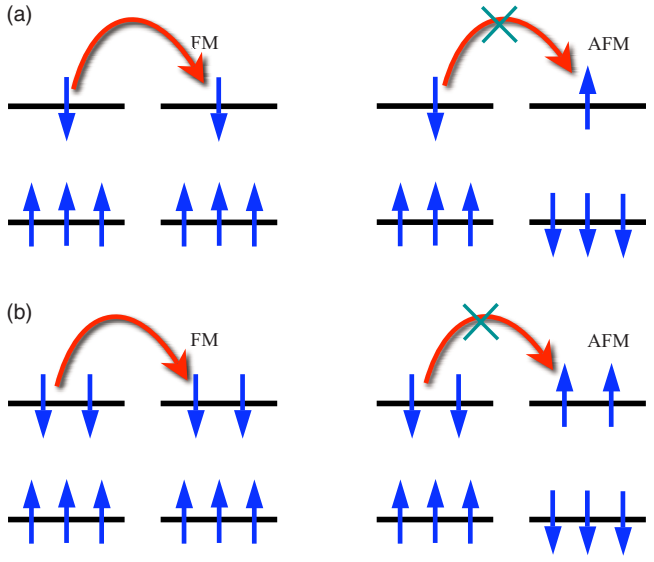

FIG. 3. (Color online) Schematic of the exchange mechanism leading to ferromagnetic coupling between defect-induced moments. Only the spin-split t_2 states are shown in the diagram. For (a) neutral as well as (b) the singly-charged cation vacancies, this virtual hopping results in an FM coupling.

the energy of the system) whereas this hopping is not allowed if the spin alignment is antiparallel. One can also explain these results within the molecular-orbital theory through the spin-conserving hopping between the bonding and antibonding states formed from the spin-split t_2 states.[61]

IV. GaN WITH POTASSIUM SUBSTITUTIONAL [GaN:K_{Ga}]

Cation vacancies are just one possibility for introducing localized defect states in systems such as ZnO and GaN. Localized defect states may also be realized by introducing acceptor like substitutionals. For example, nitrogen and carbon substitutions are predicted to give rise to local moments in ZnO.[36,45] Copper substitution in GaN is also suggested as a possible way of realizing GaN based DMS.[62–65] Although copper is normally considered as nonmagnetic, there is a possibility that its d electrons are involved in the observed magnetic behavior. Choosing potassium as a candidate example, we show that appropriate nonmagnetic cation substitutionals can also provide localized magnetic moments. In addition, we expect that the magnetic behavior of potassium substitutionals to be similar to the case of negatively charged Ga vacancies as reported in paper I.

We carry out the calculation on a 64-atom supercell containing one substitutional K. All atomic positions are fully relaxed after replacing one Ga atom with one K atom. After the relaxation, there is an outward movement of the nitrogen atoms surrounding the potassium substitutional. The K-N bond length is found to be 2.36 Å; the Ga-N bond length in the first shell around the impurity decreases from 1.95 Å (the bulk value) to 1.90 Å. In the second shell, the Ga-N bond length is slightly longer (by 0.01 Å) than the bulk value. These results are consistent with our previous study of Ga vacancy in GaN. The presence of potassium has minimal

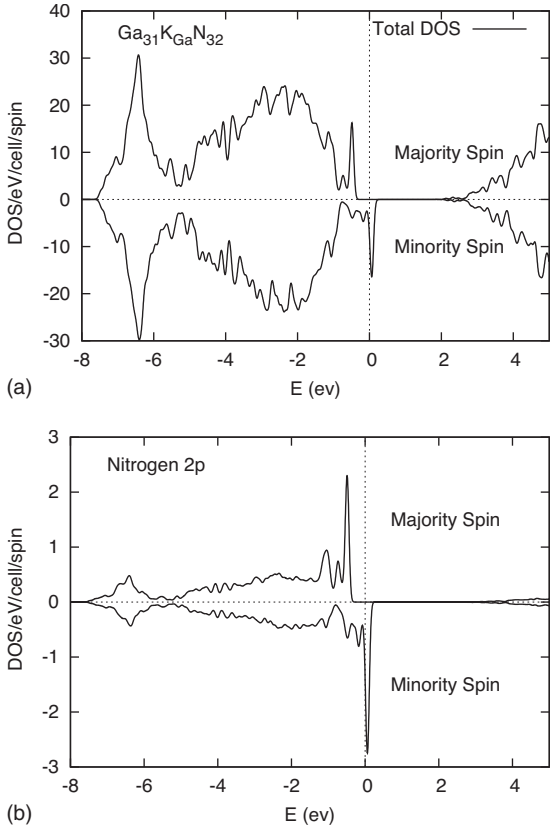

FIG. 4. (a) Spin-resolved total DOS of a K_{Ga} substitutional in a 64-atom GaN supercell. The nitrogen-2s and gallium-3d states are not shown. (b) Projection of the total DOS onto the 2p states of one of the nitrogen atoms around the defect showing that the defect states are mainly derived from the 2p states of the surrounding nitrogen.

effects on the local structural distortion and the properties of K_{Ga} should be similar to that of negatively charged Ga vacancy V_{Ga}^{-}.

Potassium substitution of Ga is a double acceptor. If the acceptor states are sufficiently localized, a spin-polarized ground state may be achieved. Our first-principles calculations confirm that a potassium substitution indeed gives rise to a $2\mu_B$ local magnetic moment per defect. Figure 4 plots the calculated spin-resolved DOS for a 64-atom GaN supercell containing one K substitutional, showing the spin-polarization effects and the formation of a net $2\mu_B$ local moment. Similar to the case of Ga vacancy in GaN, the magnetic moments are localized near the nitrogen atoms around the substitutional potassium as shown in the projected DOS in Fig. 4(b). Note that in addition to forming the defect states, 2p states of nitrogen atoms surrounding the defect also contribute to the bulk states. Therefore, the projected DOS shown in Fig. 4(b) contains both defect-state (the sharp features near the band edge) and bulk-state components.

The spin-polarization energy E_{pol} is found to be 0.23 eV per defect. The magnetic coupling between defect-induced local moment is studied using the same method described in the previous section. Table II summarizes the results of magnetic coupling between two defect-induced moments separated by 17.1 a.u. These results agree well with those of

TABLE II. Magnetic properties of K_{Ga} in GaN. The magnetic energy difference is defined in Eq. (4). The spin-polarization energy is normalized to energy per defect.

Charge state	Local moment (μ_B)	ΔE^M (meV)	J_0 (meV)	ΔE^{pol} (meV)
0	2.0	119	30	230
−1	1.0	31	31	57

charged Ga vacancy as shown in Table I. For neutral defects, from the total-energy calculations for the FM and AFM alignments of the defect-induced moments, the coupling is found to be ferromagnetic. The energy difference between the AFM state and the FM states (ΔE^M) is 119 meV. Equation (4) then yields the value of the exchange parameter to be about 30 meV, to be compared to 31 meV for the case of charged Ga vacancy as shown in Table I. The magnetic coupling can again be explained by the kinetic exchange model explained in the previous section.

V. DEFECT COMPLEX [GaN: V_{Ga}-O_N]

Substitutional oxygen is an important anion-site dopant in GaN and is often considered to be responsible for the unintentional *n*-type doping of GaN.[66,67] While oxygen substitutional is a donor, the cation vacancy is an acceptor. One would then expect that the two defects will form a stable V_{Ga}-O_N complex.[68] In fact, it was suggested that the presence of oxygen would promote the formation of Ga vacancy due to the creation of V_{Ga}-O_N complexes.[69,70] This defect complex was also proposed to be responsible for the yellow luminescence in GaN.[68,71] To our knowledge, no previous studies addressed the magnetic properties of the V_{Ga}-O_N complex.

Within the GGA, the relaxation energy (ΔE^{relax}) is calculated to be about 0.44 eV. The Ga-O bond length is 1.92 Å whereas the bond length of the Ga-N bonds around the Ga vacancy is about 1.90 Å. As discussed previously, a gallium vacancy leaves five unpaired electrons on the four N atoms surrounding the vacancy. With oxygen substituting one of the nitrogen atoms, the dangling bonds around the cation vacancy will now have six electrons, which is isoelectronic to V_{Zn} in ZnO (or K_{Ga}). Therefore, the V_{Ga}-O_N complex should result in a net local moment of $2\mu_B$. Since oxygen is more electronegative than nitrogen, one expects that the substitutional oxygen atom would form a closed-shell structure and the net magnetic moment would come from the nitrogen dangling bonds. Figure 5 shows an isosurface plot ($\rho = 8.5 \times 10^{-3}$ $e/\text{a.u}^3 = 5.7 \times 10^{22}$ e/cm^3) of the spin density ($\rho = \rho^{\uparrow} - \rho^{\downarrow}$) of the 64-atom supercell containing one V_{Ga}-O_N defect complex. It is evident that all spin moments are localized near the three nitrogen atoms around the Ga vacancy. This conclusion can also be drawn from the calculated DOS as shown in Figs. 6(a) and 6(b). Figure 6(a) shows the spin-resolved DOS of a 64-atom GaN supercell containing one V_{Ga}-O_N complex whereas Fig. 6(b) shows the projected density of states (PDOS) onto nitrogen-2*p* and the oxygen-2*p*

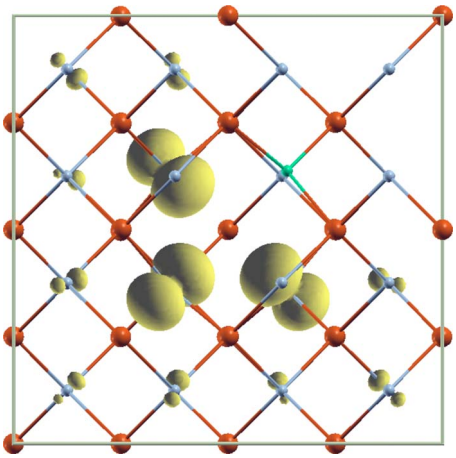

FIG. 5. (Color online) Isosurface spin-density plot ($\rho = \rho^{\uparrow} - \rho^{\downarrow} = 8.5 \times 10^{-3}$ $e/\text{a.u.}^3$) for V_{Ga}-O_N in GaN. The red balls (dark gray) are gallium atoms, the blue (light gray) are nitrogen atoms, and the green (very light gray) is the oxygen substitutional replacing one of the nitrogen atoms surrounding the vacancy. The cation vacancy is located at the center of the supercell.

states. The defect states near the band edge are mostly derived from the nitrogen-*p* states while the oxygen-*p* states are resonant with bulk states. Therefore, it is the 2*p* electrons of the three nitrogen atoms surrounding the vacancy site that mostly furnish the defect's magnetic moment.

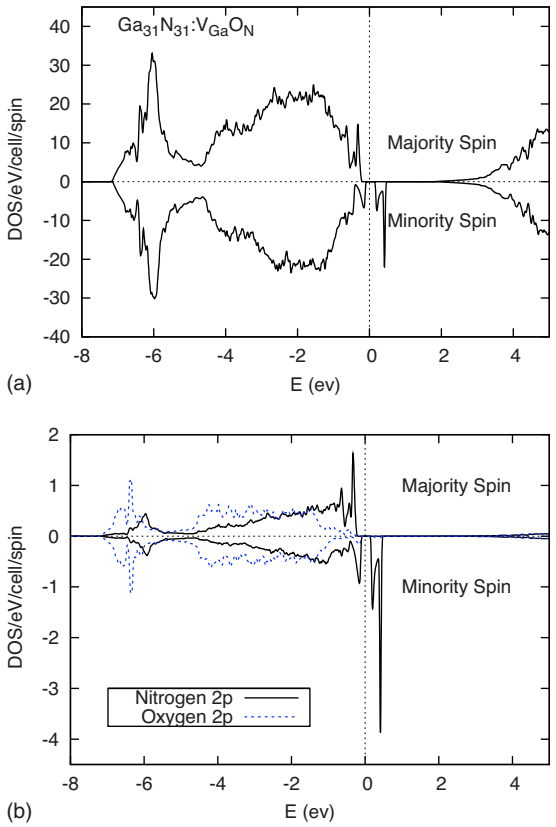

FIG. 6. (Color online) (a) Spin-resolved total DOS and (b) projected DOS of a V_{Ga}-O_N complex in 64-atom GaN supercell. The projection is carried out for the 2*p* states of the substitutional oxygen atom and one of the nitrogen atom around the vacancy.

TABLE III. Magnetic coupling between the defect-induced local moments in [GaN:V_{Ga}-O_N]. The magnetic energy difference is defined in Eq. (4). The spin-polarization energy is normalized to energy per defect.

Charge state	Local moment (μ_B)	ΔE^M (meV)	J_0 (meV)	ΔE^{pol} (meV)
0	2.0	−4.5	−1.1	382
−1	1.0	54	54	133

Next, we address the issue of magnetic coupling between defect-induced moments. Since the V_{Ga}-O_N complex is isoelectronic to K_{Ga}, one might naïvely expect that the magnetic coupling between the two defect-induced moments to be ferromagnetic, similar to that for K_{Ga}. However, instead of being ferromagnetic, the magnetic coupling between the neutral defect complexes is found to be weakly antiferromagnetic (J_0=−1.1 meV) as shown in Table III. Interestingly, charging the defect complex recovers a strong ferromagnetic coupling.

To understand the nature of the magnetic coupling, one needs to examine the energy levels of this defect complex, as shown in Fig. 7. Upon oxygen substitution, the symmetry of the system is reduced from the T_d symmetry to a lower C_{3v} symmetry. Under the T_d symmetry, the sp^3 states split into a singlet (a_1) and a triplet (t_2) state. The singlet a_1 lies very low in energy and we will not concern ourselves with it in the following discussion. Under the actual C_{3v} symmetry, the crystal field further splits the t_2 state into a doublet (e) and a singlet (a_1). The spin polarization then lifts the spin degeneracy. The resulting energy diagram for the t_2-derived defect states is shown schematically in Fig. 7. Therefore, the four electrons are distributed among these t_2-derived states and a net magnetic-moment results from the half-filled e states.

There are several interesting features in the defect level diagram shown in Fig. 7. First, due to the crystal-field splitting (arising from both the local structural distortion and oxygen potential), the low-energy defect levels now consist of a fully filled a_1 state and a half-filled e state. As a result, an energy gap develops between the minority a_1 and e states, which can also be seen in Fig. 6. This explains the antiferromagnetic nature of the exchange coupling as shown in Fig. 8. Virtual hopping from the occupied e states to the same-spin unoccupied e states results in a AFM coupling between the defect complexes. Second, the spin splitting between the majority- and minority-spin e states is very large (~1.4 eV), which is substantially larger than that for a simple Ga vacancy (about 0.6 eV). This big spin splitting is largely responsible for the fairly weak antiferromagnetic coupling since the magnetic coupling scales as $t^2/(U+\Delta\epsilon)$, where t is the nearest-neighbor hopping matrix element, U is the on-site Coulomb energy, and $\Delta\epsilon$=1.4 eV is the spin splitting. Therefore, it is this delicate interplay between the spin splitting and the crystal-field splitting that results in a rather weak antiferromagnetic exchange coupling.

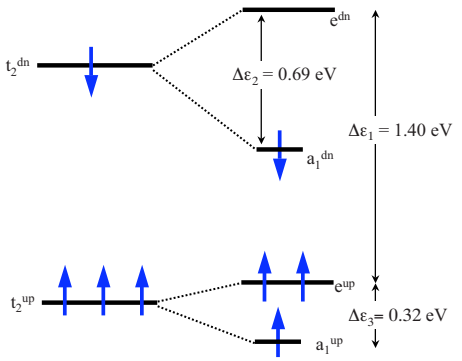

FIG. 7. (Color online) Schematic of the defect levels for V_{Ga}-O_N. The majority- and minority-spin t_2 states split into the singlet a_1 and the doublet e states under the C_{3v} symmetry, resulting in a completely filled a_1 and a half-filled e states.

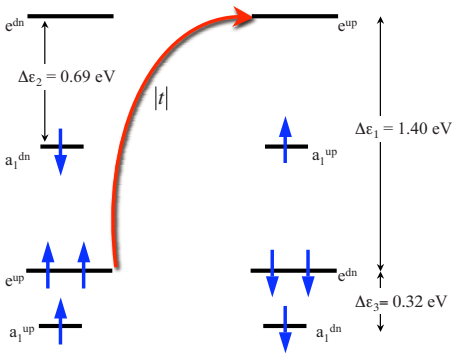

FIG. 8. (Color online) Virtual hopping between the defect states for V_{Ga}-O_N in GaN, resulting in a weak AFM coupling between defect-induced moments.

The V_{Ga}-O_N complex is a double acceptor and can exist in different charge states. Therefore, we have also studied the magnetic properties of singly-charged defect complex. Not surprisingly, a partial compensation of the acceptor results in a strong ferromagnetic coupling between the defect-induced local moments (Table III). The ferromagnetic coupling can again be understood within the kinetic hopping as shown in Fig. 9. The virtual hopping between the partially filled minority-spin doublets (e state) lowers the energy when local spins have parallel alignment while such hopping is not allowed when the spins are antiparallel to each other.

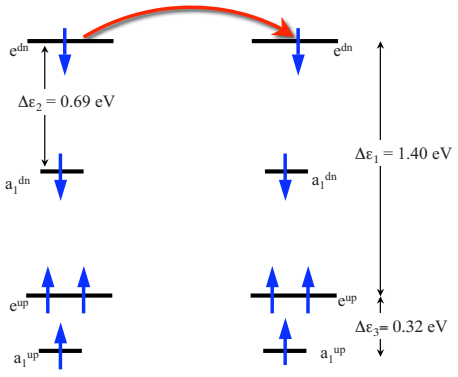

FIG. 9. (Color online) Virtual hopping between the charged defect states for V_{Ga}-O_N in GaN which explains the FM coupling between defect-induced moments.

VI. DISCUSSION

It is well known that defects play an important role in controlling electronic, optical, transport, interface and surface properties of the materials. Through this work, we wish to emphasize that defects, especially localized defects such as acceptors in II-oxides and III-nitrides, might also play an important role in controlling the magnetic properties of these otherwise nonmagnetic semiconductors. Local moment formation is a result of the localized "nonmagnetic" defect states. The extended tails of the defect wave function could mediate long-ranged magnetic couplings. In addition to the defects studied in this work, other candidates that might lead to the observed magnetism include those studied by Mitra and Lambrecht.[72]

In the case of oxide- and nitride-based DMS containing magnetic impurities, both nonmagnetic (intrinsic and extrinsic) defects and magnetic impurities may contribute to the observed magnetism. In addition, different exchange mechanism may contribute to the magnetic coupling among these local moments. Magnetic exchange may originate from the coupling between extrinsic impurities and the intrinsic defect states, between intrinsic defects, and between extrinsic magnetic impurities. As mentioned in Sec. I, there are numerous experimental reports on magnetic behavior of semiconductors possessing only intrinsic or other nonmagnetic extrinsic defects. Understanding the magnetic behavior of "nonmagnetic" defects is thus an important step toward a better understanding and control of properties of the doped DMS. Experimentally, we expect that defects are most likely randomly distributed. Therefore, a full understanding of the defect-induced magnetism can only be obtained by mapping out both the distance and angle dependence of the exchange parameters. In fact, in an earlier work,[23] we investigated the distance dependence of the magnetic coupling by studying the magnetic coupling parameters at two distances for GaN and BN. Significant magnetic coupling was found for defect separation as large as 25.6 a.u. However, the precise form for the decay of the exchange coupling parameters has not been mapped out. It is our intention to continue this work to study both distance and orientation dependence of the magnetic coupling in these systems with the hope to find a simple functional form for it.

It should also be pointed out that defect-induced magnetism is a subject of considerable complexity. Precisely what kinds of defects—vacancies, acceptor impurities, or defect complexes—are present and are responsible for the magnetism in various samples will depend on the growth conditions and post-growth treatments. For example, in the carbon-doped ZnO, it is likely that the C-substitutionals play a major role. However, in the samples with no intentional doping, vacancies might be responsible for the observed magnetism. Acceptor impurities and complexes usually have lower formation energy than vacancies and as a result of this, might become the dominant defects in the system. However, if the defects are created using highly nonequilibrium techniques, formation energy of defects may not be a concern. Instead, the dynamics of defects creation and their stability might be more important. This is a subject we have not explored here. Moreover, the nature of the magnetic coupling between defect-induced moments, i.e., ferromagnetic or antiferromagnetic, long-ranged or short-ranged, is a result of delicate interplay between local structural distortion, defect level splitting, and localization of defect wave functions. Therefore, one has to be cautious in making a general conclusion. In addition to the aforementioned considerations, the nature and strength of the magnetic coupling between local moments are themselves dependent on the defects' charge state. This charge-state sensitivity of the magnetic coupling may prove to be both a challenge as well as an opportunity and may open up new routes toward tuning and controlling the magnetic coupling by optical, charge, or thermal excitations.[73–75]

There is an additional complication that impedes the theoretical understanding of defect-induced magnetism. Standard DFT-based methods sometime encounter difficulties in treating localized defect states and might underestimate local structural distortions and localization of defect wave functions. More accurate treatment of the electron correlation effects for localized defect states is certainly a subject of great importance and deserves a more careful investigation.[76–78] Given the convincing experimental evidence of magnetism in undoped semiconductors, an in-depth understanding of defect-induced magnetism is imperative and should, in turn, help to make better, more consistent high-T_C DMS by careful manipulation of defects.

ACKNOWLEDGMENT

We acknowledge the computational support provided by the Center for Computational Research at the University at Buffalo, SUNY. This work is supported by the Department of Energy under Grant No. DE-SC0002623.

[1] K. Ando, Science **312**, 1883 (2006).
[2] T. Dietl, H. Ohno, F. Matsukura, J. Cibert, and D. Ferrand, Science **287**, 1019 (2000).
[3] A. M. Nazmul, S. Sugahara, and M. Tanaka, Phys. Rev. B **67**, 241308(R) (2003).
[4] C. Liu, F. Yun, and H. Morkoç, J. Mater. Sci.: Mater. Electron. **16**, 555 (2005).
[5] M. E. Overberg, C. R. Abernathy, S. J. Pearton, N. A. Theodoropoulou, K. T. McCarthy, and A. F. Hebard, Appl. Phys. Lett. **79**, 1312 (2001).
[6] T. Sasaki, S. Sonoda, Y. Yamamoto, K. Suga, S. Shimizu, K. Kindo, and H. Hori, J. Appl. Phys. **91**, 7911 (2002).
[7] M. L. Reed, N. A. El-Masry, H. H. Stadelmaier, M. K. Ritums, M. J. Reed, C. A. Parker, J. C. Roberts, and S. M. Bedair, Appl. Phys. Lett. **79**, 3473 (2001).
[8] V. A. Chitta, J. A. H. Coaquira, J. R. L. Fernandez, C. A. Duarte, J. R. Leite, D. Schikora, D. J. As, K. Lischka, and E. Abramof, Appl. Phys. Lett. **85**, 3777 (2004).

[9] N. H. Hong, V. Brizé, and J. Sakai, Appl. Phys. Lett. **86**, 082505 (2005).
[10] K. Ueda, H. Tabata, and T. Kawai, Appl. Phys. Lett. **79**, 988 (2001).
[11] X. C. Liu, E. W. Shi, Z. Z. Chen, H. W. Zhang, B. Xiao, and L. X. Song, Appl. Phys. Lett. **88**, 252503 (2006).
[12] T. Fukumura, Z. Jin, M. Kawasaki, T. Shono, T. Hasegawa, S. Koshihara, and H. Koinuma, Appl. Phys. Lett. **78**, 958 (2001).
[13] X. M. Cheng and C. L. Chien, J. Appl. Phys. **93**, 7876 (2003).
[14] I. S. Elfimov, S. Yunoki, and G. A. Sawatzky, Phys. Rev. Lett. **89**, 216403 (2002).
[15] J. Osorio-Guillén, S. Lany, S. V. Barabash, and A. Zunger, Phys. Rev. Lett. **96**, 107203 (2006).
[16] C. H. Patterson, Phys. Rev. B **74**, 144432 (2006).
[17] H. Liu, X. Zhang, L. Li, Y. X. Wang, K. H. Gao, Z. Q. Li, R. K. Zheng, S. P. Ringer, B. Zhang, and X. X. Zhang, Appl. Phys. Lett. **91**, 072511 (2007).
[18] C. Song, S. N. Pan, X. J. Liu, X. W. Li, F. Zeng, W. S. Yan, B. He, and F. Pan, J. Phys.: Condens. Matter **19**, 176229 (2007).
[19] D. Iuşan, B. Sanyal, and O. Eriksson, Phys. Status Solidi **204**, 53 (2007).
[20] D. C. Mattis, *The Theory of Magnetism* (Harper and Row, New York, 1965).
[21] T. A. Kennedy, N. D. Wilsey, J. J. Krebs, and G. H. Stauss, Phys. Rev. Lett. **50**, 1281 (1983).
[22] P. Mahadevan and S. Mahalakshmi, Phys. Rev. B **73**, 153201 (2006).
[23] P. Dev, Y. Xue, and P. Zhang, Phys. Rev. Lett. **100**, 117204 (2008).
[24] Y. Zhang, S. Talapatra, S. Kar, R. Vajtai, S. K. Nayak, and P. M. Ajayan, Phys. Rev. Lett. **99**, 107201 (2007).
[25] F. Máca, J. Kudrnovský, V. Drchal, and G. Bouzerar, Appl. Phys. Lett. **92**, 212503 (2008).
[26] Q. Wang, Q. Sun, G. Chen, Y. Kawazoe, and P. Jena, Phys. Rev. B **77**, 205411 (2008).
[27] T. L. Makarova, B. Sundqvist, R. Höhne, P. Esquinazi, Y. Kopelevichk, P. Scharff, V. A. Davydov, L. S. Kashevarova, and A. V. Rakhmanina, Nature (London) **413**, 716 (2001).
[28] R. A. Wood, M. H. Lewis, M. R. Lees, S. M. Bennington, M. G. Cain, and N. Kitamura, J. Phys.: Condens. Matter **14**, L385 (2002).
[29] J. M. D. Coey, M. Venkatesan, C. B. Fitzgerald, A. P. Douvalis, and I. S. Sanders, Nature (London) **420**, 156 (2002).
[30] P. Esquinazi, D. Spemann, R. Höhne, A. Setzer, K.-H. Han, and T. Butz, Phys. Rev. Lett. **91**, 227201 (2003).
[31] S. Talapatra, P. G. Ganesan, T. Kim, R. Vajtai, M. Huang, M. Shima, G. Ramanath, D. Srivastava, S. C. Deevi, and P. M. Ajayan, Phys. Rev. Lett. **95**, 097201 (2005).
[32] H. Ohldag, T. Tyliszczak, R. Höhne, D. Spemann, P. Esquinazi, M. Ungureanu, and T. Butz, Phys. Rev. Lett. **98**, 187204 (2007).
[33] C. B. Fitzgerald, M. Venkatesan, L. S. Dorneles, R. Gunning, P. Stamenov, J. M. D. Coey, P. A. Stampe, R. J. Kennedy, E. C. Moreira, and U. S. Sias, Phys. Rev. B **74**, 115307 (2006).
[34] M. Venkatesan, C. B. Fitzgerald, and J. M. D. Coey, Nature (London) **430**, 630 (2004).
[35] N. H. Hong, J. Sakai, N. Poirot, and V. Brizé, Phys. Rev. B **73**, 132404 (2006).
[36] H. Pan, J. B. Yi, L. Shen, R. Q. Wu, J. H. Yang, J. Y. Lin, Y. P. Feng, J. Ding, L. H. Van, and J. H. Yin, Phys. Rev. Lett. **99**, 127201 (2007).
[37] N. H. Hong, J. Sakai, N. T. Huong, N. Poirot, and A. Ruyter, Phys. Rev. B **72**, 045336 (2005).
[38] K. Kusakabe and M. Maruyama, Phys. Rev. B **67**, 092406 (2003).
[39] Y.-H. Kim, J. Choi, K. J. Chang, and D. Tománek, Phys. Rev. B **68**, 125420 (2003).
[40] J. A. Chan, B. Montanari, J. D. Gale, S. M. Bennington, J. W. Taylor, and N. M. Harrison, Phys. Rev. B **70**, 041403(R) (2004).
[41] A. N. Andriotis, R. M. Sheetz, E. Richter, and M. Menon, Europhys. Lett. **72**, 658 (2005).
[42] O. V. Yazyev and L. Helm, Phys. Rev. B **75**, 125408 (2007).
[43] C. Das Pemmaraju and S. Sanvito, Phys. Rev. Lett. **94**, 217205 (2005).
[44] S. W. Fan, K. L. Yao, Z. L. Liu, G. Y. Gao, Y. Min, and H. G. Cheng, J. Appl. Phys. **104**, 043912 (2008).
[45] L. Shen, R. Q. Wu, H. Pan, G. W. Peng, M. Yang, Z. D. Sha, and Y. P. Feng, Phys. Rev. B **78**, 073306 (2008).
[46] J. P. Perdew and Y. Wang, Phys. Rev. B **33**, 8800 (1986).
[47] J. P. Perdew, K. Burke, and M. Ernzerhof, Phys. Rev. Lett. **77**, 3865 (1996).
[48] S. Baroni *et al.*, http://www.pwscf.org/; URL http://www.pwscf.org/
[49] D. R. Hamann, M. Schlüter, and C. Chiang, Phys. Rev. Lett. **43**, 1494 (1979).
[50] D. Vanderbilt, Phys. Rev. B **41**, 7892 (1990).
[51] H. J. Monkhorst and J. D. Pack, Phys. Rev. B **13**, 5188 (1976).
[52] E. Martinez-Guerrero *et al.*, J. Appl. Phys. **91**, 4983 (2002).
[53] S.-M. Zhou, H.-C. Gong, B. Zhang, Z.-L. Du, X.-T. Zhang, and S.-X. Wu, Nanotechnology **19**, 175303 (2008).
[54] M. Oshikiri and F. Aryasetiawan, Phys. Rev. B **60**, 10754 (1999).
[55] L. Ley, R. A. Pollak, F. R. McFeely, S. P. Kowalczyk, and D. A. Shirley, Phys. Rev. B **9**, 600 (1974).
[56] V. I. Anisimov, F. Aryasetiawan, and A. I. Lichtenstein, J. Phys.: Condens. Matter **9**, 767 (1997).
[57] V. Fernandes *et al.*, Phys. Rev. B **80**, 035202 (2009).
[58] S. Zhang, S. B. Ogale, W. Yu, X. Gao, T. Liu, S. Ghosh, G. P. Das, A. T. S. Wee, R. L. Greene, and T. Venkatesan, Adv. Mater. **21**, 2282 (2009).
[59] M. Khalid *et al.*, Phys. Rev. B **80**, 035331 (2009).
[60] A. N. Yaresko, A. Y. Perlov, R. Hayn, and H. Rosner, Phys. Rev. B **65**, 115111 (2002).
[61] P. Mahadevan, A. Zunger, and D. D. Sarma, Phys. Rev. Lett. **93**, 177201 (2004).
[62] R. Q. Wu, G. W. Peng, L. Liu, Y. P. Feng, Z. G. Huang, and Q. Y. Wu, Appl. Phys. Lett. **89**, 062505 (2006).
[63] H.-K. Seong, J.-Y. Kim, J.-J. Kim, S.-C. Lee, S.-R. Kim, U. Kim, T.-E. Park, and H.-J. Choi, Nano Lett. **7**, 3366 (2007).
[64] H. J. Xiang and S.-H. Wei, Nano Lett. **8**, 1825 (2008).
[65] X. L. Yang, Z. T. Chen, C. D. Wang, Y. Zhang, X. D. Pei, Z. J. Yang, G. Y. Zhang, Z. B. Ding, K. Wang, and S. D. Yao, J. Appl. Phys. **105**, 053910 (2009).
[66] B.-C. Chung and M. Gershenzon, J. Appl. Phys. **72**, 651 (1992).
[67] H. Sato, T. Minami, E. Yamada, M. Ishii, and S. Takata, J. Appl. Phys. **75**, 1405 (1994).
[68] J. Neugebauer and C. G. Van de Walle, Appl. Phys. Lett. **69**, 503 (1996).
[69] J. Oila *et al.*, Phys. Rev. B **63**, 045205 (2001).
[70] S. Hautakangas, I. Makkonen, V. Ranki, M. J. Puska, K. Saarinen, X. Xu, and D. C. Look, Phys. Rev. B **73**, 193301

(2006).
[71] J. Jenny, R. Jones, J. E. V. Nostrand, D. C. Reynolds, D. C. Look, and B. Jogai, Solid State Commun. **106**, 701 (1998).
[72] C. Mitra and W. R. L. Lambrecht, Phys. Rev. B **80**, 081202(R) (2009).
[73] R. Beaulac, L. Schneider, P. I. Archer, G. Bacher, and D. R. Gamelin, Science **325**, 973 (2009).
[74] S. T. Ochsenbein, Y. Feng, K. M. Whitaker, E. Badaeva, W. K. Liu, X. Li, and D. R. Gamelin, Nat. Nanotechnol. **4**, 681 (2009).
[75] S. Mishra, G. S. Tripathi, and S. Satpathy, Phys. Rev. B **77**, 125216 (2008).
[76] A. Droghetti, C. D. Pemmaraju, and S. Sanvito, Phys. Rev. B **78**, 140404(R) (2008).
[77] S. Lany and A. Zunger, Phys. Rev. B **80**, 085202 (2009).
[78] J. A. Chan, S. Lany, and A. Zunger, Phys. Rev. Lett. **103**, 016404 (2009).